CRREL REPORT 94-1

Growth Condition of an Ice Layer in Frozen Soils Under Applied Loads

2: Analysis

Yoshisuke Nakano and Kazuo Takeda

January 1994

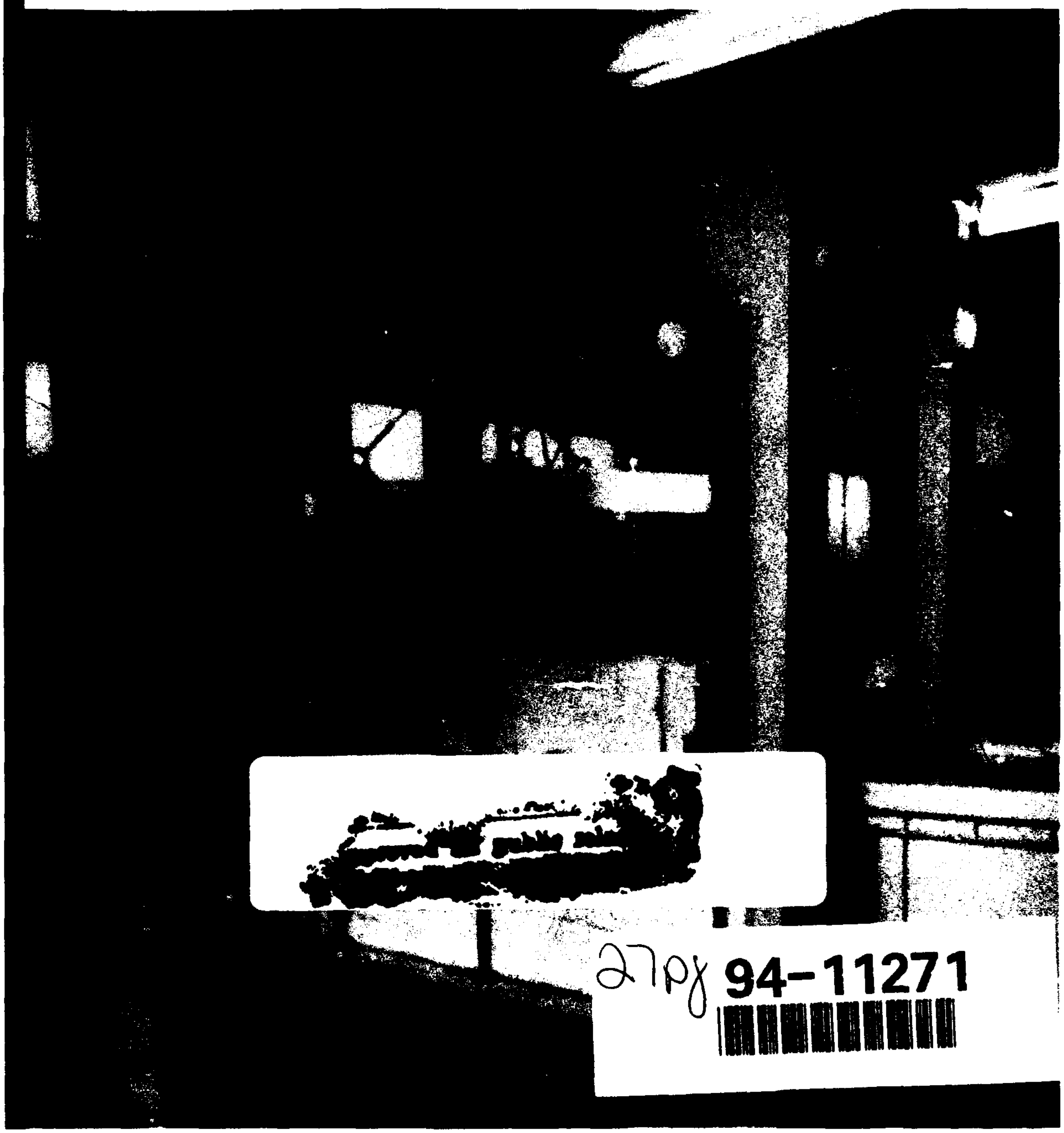

Abstract

The results of an experimental study on the steady growth condition of a segregated ice layer under various applied pressures were presented in Part 1. Using the data obtained, we evaluate the accuracy of the model M_1, and the predicted steady growth condition is found to be in good agreement with the condition found empirically. The concept of segregation potential introduced by Konrad and Morgenstern in the early 1980s is examined based on M_1. M_1 is found to be consistent with the empirical data that were used to support their segregation potential theory.

Cover: Apparatus for testing ice growth in soils under applied loads. (Photo by K. Takeda.)

For conversion of SI metric units to U.S./British customary units of measurement consult *Standard Practice for Use of the International System of Units (SI)*, ASTM Standard E380-89a, published by the American Society for Testing and Materials, 1916 Race St., Philadelphia, Pa. 19103.

CRREL Report 94-1

US Army Corps of Engineers
Cold Regions Research & Engineering Laboratory

Growth Condition of an Ice Layer in Frozen Soils Under Applied Loads

2: Analysis

Yoshisuke Nakano and Kazuo Takeda

January 1994

Accesion For	
NTIS CRA&I	☒
DTIC TAB	☐
Unannounced	☐
Justification	
By	
Distribution /	
Availability Codes	
Dist	Avail and / or Special
A-1	

Prepared for
OFFICE OF THE CHIEF OF ENGINEERS

Approved for public release; distribution is unlimited.

PREFACE

This report was prepared by Dr. Yoshisuke Nakano, Chemical Engineer, of the Applied Research Branch, Experimental Engineering Division, U. S. Army Cold Regions Research and Engineering Laboratory, and by Dr. Kazuo Takeda of the Technical Research Institute, Konoike Construction Co., Ltd., Konohana, Osaka, Japan. Funding for Dr. Nakano's research was provided by DA Project 4A161102AT24, *Research in Snow, Ice and Frozen Ground*, Task SC, Work Unit F01, *Physical Processes in Frozen Soil*. Dr. Takeda's experimental work was funded by Konoike Construction Company.

The authors thank Dr. Virgil Lunardini and Dr. Y.C. Yen of CRREL for their technical review of this report.

The contents of this report are not to be used for advertising or promotional purposes. Citation of brand names does not constitute an official endorsement or approval of the use of such commercial products.

CONTENTS

ILLUSTRATIONS

TABLES

NOMENCLATURE

a function defined by eq 11a

a_e function defined by eq 27f

a_i constant where i = 0, 1, ... 3

$\hat{a}_i$ function defined by eq 25d and 25e, where $i = 0, 1$

A constant

b function defined by eq 11b

b_i constant where $i = 1,2$.

B_i ith constituent of the mixture. Subscripts $i = 1, 2$, and 3 are used to denote unfrozen water, ice and soil minerals, respectively

c_i heat capacity of the ith constituent

d unit of time (day)

d_i density of the *i*th constituent

e void ratio

f_i mass flux of the *i*th constituent relative to that of soil minerals where $i = 1, 2$

f_{10} mass flux of water in the unfrozen part of the soil

I function defined by eq 16b

k thermal conductivity of a frozen fringe defined by eq 9a

k_0 thermal conductivity of the unfrozen part of the soil

k_1 thermal conductivity of an ice layer

k_{01} limiting value of k defined by eq 9c

K_0 hydraulic conductivity in the unfrozen part of the soil

K_i empirical function defined by eq 4a where $i = 1, 2$

K_{i1} limiting value of K_i as x approaches n_1 while x is in R_1, $i = 1,2$

K_{i0} limiting value of K_i as x approaches n_0 while x is in R_1, $i = 1,2$

L latent heat of fusion of water, 334 J g^{-1}

m location of the free end of the column

M_i name of a model where $i = 1, 2, 3$

n boundary in R_0

n_i boundary with $i = 0, 1$ where n_0 denotes the boundary where $T = 0°C$ and n_1 the interface between an ice layer and a frozen fringe

n_{10} boundary between R_{10} and R_{11}

p_0 gravity term, 0.098 [kPa/cm]

P_i pressure of the *i*th constituent where $i = 1, 2$

P_{10} value of P_1 at n_0

P_{1n} value of P_1 at n

P_{21} value of P_2 at n_1

r rate of heave

R_0 unfrozen part of the soil

R_1 frozen fringe

R_{10} part of the soil bounded by n_0 and n_{10}

R_{11} essential frozen fringe

R_2 ice layer

R_m region in the diagram of temperature gradients where an ice layer melts

R_s region in the diagram of temperature gradients where the steady growth of an ice layer occurs

R_s^* boundary between R_s and R_u

R_s^{**} boundary between R_m and R_s

R_u region in the diagram of temperature gradients where the steady growth of an ice layer does not occur

S property of a given soil

SP_0 segregation potential defined by eq 2a

t time

T temperature

T_1 temperature at n_1

T_{10} defined by eq 41

T_{11} calculated value of T_1 from the measured temperature profile in R_2

$\widehat{T}_1^*$ empirically determined value of T_1^*

T_1^{**} temperature at n_1 when eq 1 holds true

$\widehat{T}_0$ constant

$(T')_a$ average temperature gradient in R_1

ΔT defined by eq 3c

x spatial coordinate

y variable defined by eq 17c

$\bar{y}$ variable defined by eq 38b

y_a variable defined by eq 3a

$\alpha(t)$ trajectory $[\alpha_1(t), \alpha_0(t)]$ in the diagram of temperature gradients

α_0 absolute value of the temperature gradient at n_0

α_1 absolute value of the limiting temperature gradient as x approaches n_1 while x is in R_2, defined by eq 6

α_f absolute value of the temperature gradient near n_1 in R_2

α_u absolute value of the temperature gradient near n_0 in R_0

β_0 defined by eq 11c

γ constant, 1.12 MPa °C^{-1}

γ_1 defined by eq 24b

δ thickness of a frozen fringe

δ^{**} defined by eq 27b

δ_e thickness of an essential frozen fringe defined by eq 27a

δ_0 defined by eq 13c

η defined by eq 9b

ρ composition of the soil

ρ_i bulk density of the *i*th constituent

σ effective pressure defined by eq 1 and 16c

ϕ_0 empirical function of T defined by eq 14a

ϕ_{01} value of ϕ_0 at $T = T_1$

ϕ_1 empirical function of T defined by eq 14b

ϕ_{11} value of ϕ_1 at $T = T_1$

φ_0 variable defined by eq 21b

φ_1 variable defined by eq 25f

ω_i dimensionless quantity defined by eq.18a through 18d where $i = 0, 1, ..., 3$

i subscript denotes the *i*th constituent of the mixture consisting of unfrozen water ($i = 1$), ice ($i = 2$) and soil minerals ($i = 3$)

* superscript used to indicate the value of any variable evaluated when a point (α_1, α_0) in the diagram of temperature gradients is on R_s^*

** superscript used to indicate the value of any variable evaluated when a point (α_1, α_0) in the diagram of temperature gradients is on R_s^{**}

Growth Condition of an Ice Layer in Freezing Soils Under Applied Loads
2. Analysis

YOSHISUKE NAKANO AND KAZUO TAKEDA

INTRODUCTION

In this report we will consider the one-directional steady growth of an ice layer. Let the freezing process advance from the top down and the coordinate x be positive upwards, with its origin fixed at some point in the unfrozen part of the soil. A freezing soil in this problem may be considered to consist of three parts: the unfrozen part R_0, the frozen fringe R_1 and the ice layer R_2, as shown in Figure 1. The physical properties of parts R_0 and R_2 are well understood but our knowledge on the physical properties and the dynamic behavior of part R_1 does not appear sufficient for engineering applications.

It has been shown empirically (Radd and Oertle 1973, Takashi et al. 1981) that there is a unique temperature T_1^{**} at n_1 for a given pressure of ice P_{21} at n_1 and a given pressure of water P_1 in R_0 when an existing ice layer neither grows nor melts and the mass flux of water f_1 in R_1 vanishes. This temperature T_1^{**} at the phase equilibrium of water is given as

$$\sigma = P_{21} - P_1 = -\gamma T_1^{**}, \qquad \text{if} \qquad f_1 = 0 \tag{1}$$

where γ is a constant with the value of 1.12 MPa °C^{-1}, and σ and P_{21} are often referred to as the effective pressure and the overburden pressure, respectively. Equation 1 is often called the generalized Clausius-Clapeyron equation, which is attributed to Edlefsen and Anderson (1943).

Konrad and Morgenstern (1980, 1981, 1982) empirically found that the rate of water intake f_{10} at the formation of the final ice lens is proportional to the average temperature gradient $(T')_a$ in the frozen fringe. This may be written as

$$f_{10} = -SP_0(T')_a \tag{2a}$$

where a prime denotes differentiation with respect to x. The positive proportionality factor SP_0 is termed the segregation potential, which is a property of a given soil. Konrad and Morgenstern also found empirically that SP_0 is a decreasing function of both the applied pressure σ and the suction of water ($-P_{10}$) at n_0. We will write this dependence as

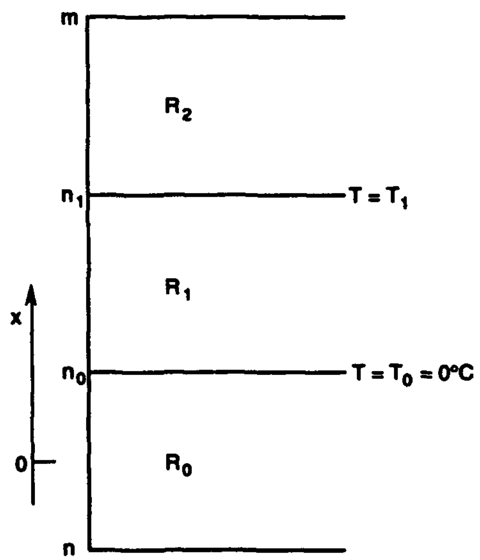

Figure 1. Schematic of a steadily growing ice layer in a freezing soil.

erally depend on the temperature T and the composition of the soil. We will describe such functional dependence of K_i ($i = 1,2$) as

$$K_1 = K_1(T, \rho) \tag{4d}$$

$$K_2 = K_2(T, \rho) \tag{4e}$$

where ρ symbolically denotes the composition of the soil that is uniquely determined by the bulk densities of unfrozen water ρ_1, ice ρ_2 and soil minerals ρ_3.

Nakano (1990) obtained the exact mathematical solution to the problem of a steadily growing ice layer based on the model M_1. Analyzing the behavior of this solution, we showed that M_1 is consistent with eq 1 (Nakano 1990) and eq 3b (Nakano and Takeda 1991). We also showed (Nakano and Takeda 1991) that M_1 can accurately describe the steady growth condition of an ice layer under negligible applied pressures.

The steady growth condition of an ice layer with or without applied pressure is the region R_s bounded by a curve R_s^* and a straight line R_s^{**} in the diagram of temperature gradients as shown in Figure 3. The region R_s is defined as

$$(k_1/k_0)\alpha_1 > \alpha_0 > k_1\,(k_0 + LbK_{21}^*)^{-1}\,\alpha_1 \tag{5}$$

where k_1 and k_0 are the thermal conductivities of R_2 and R_0, respectively, α_0 is the absolute value of the temperature gradient at n_0 and α_1 is the limiting value of the temperature gradient at n_1 in R_2 defined as

$$\alpha_1 = -\lim_{\substack{x \to n_1 \\ x \text{ in } R_2}} T'(x). \tag{6}$$

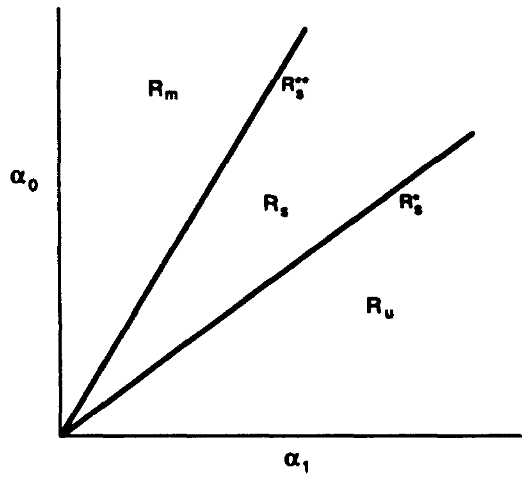

Figure 3. Temperature gradients α_1 and α_0.

In eq 5, L is the latent heat of fusion of water, b is a function of the thickness δ of R_1 defined by eq 73c and 73e in Nakano (1990), and K_{21} is the limiting value of K_2 as x approaches n_1 when x is in R_1 and an asterisk denotes that K_{21}^* is the value of K_{21} when a point (α_1, α_0) is on R_s^* in the diagram of temperature gradients.

In Figure 3 we will refer to the region as R_m where $\alpha_0 > (k_1/k_0)\alpha_1$, $f_{10} < 0$ and an ice layer is melting. The boundary R_s^{**} is given as

$$\alpha_0 = (k_1/k_0)\,\alpha_1 \qquad \text{on } R_s^{**}. \tag{7a}$$

An existing ice layer neither grows no melts, f_{10} vanishes and eq 1 holds true on R_s^{**}. The boundary R_s^* is given as

$$\alpha_0 = k_1\left(k_0 + LbK_{21}^*\right)^{-1}\alpha_1 \qquad \text{on } R_s^*. \tag{7b}$$

It is easy to see from eq 5 that the steady growth condition of a given soil is uniquely determined by α_1 and α_0. Nakano (1990) showed that all physical variables such as f_{10}, T_1, δ, etc., are also uniquely determined by α_1 and α_0 for given hydraulic conditions, and applied pressure σ. The hydraulic condition in our tests is specified by the distance δ_0 between n_0 and n where the pressure P_{1_n} of water is kept at the atmospheric pressure. Therefore, any point in R_s is uniquely specified by α_1 and α_0 for given δ_0, P_{1_n} and σ. We will write this as

$$R_s = R_s(\alpha_1, \alpha_0; \quad \delta_0, P_{1_n}, \sigma). \tag{8a}$$

Since α_1 and α_0 are related by eq 7b on R_s^*, any point on R_s^* is uniquely specified by either α_1 or α_0 for given δ_0, P_{1_n} and σ as

$$R_s^* = R_s^*(\alpha_0; \quad \delta_0, P_{1_n}, \sigma). \tag{8b}$$

The main objective of this work is to show that M_1 is consistent with the data under various applied pressures that were presented in Part I. We will also show that M_1 is consistent with the reported empirical equations such as eq 2a–c and 3b–c. Furthermore, we will evaluate the concept of segregation potential introduced by Konrad and Morgenstern (1980, 1981, 1982) based on M_1 and experimental data.

PROPERTIES OF M_1

Treating a given soil as a mixture of water in liquid phase B_1, ice B_2 and soil minerals B_3, Nakano (1990) obtained the exact mathematical solution to the problem of a steadily growing ice layer based on the model M_1 under the following assumptions. The density of each constituent remains constant, the dry density of R_0 remains constant, the part R_0 is kept saturated with water at all times and the pressure of water P_{1_n} at some boundary n fixed in R_0 remains constant. The thermal conductivity $k(x)$ in R_1 is assumed to be a nondecreasing linear function of x given as

$$k(x) = k_0[1 + \eta(x - n_0)], \qquad n_1 > x \geq n_0 \tag{9a}$$

$$\eta = (k_{01} - k_0)/(\delta k_0) \tag{9b}$$

$$\lim_{\substack{x \to n_1 \\ x \text{ in } R_1}} k = k_{01} \leq k_1 \tag{9c}$$

$$\delta = n_1 - n_0. \tag{9d}$$

The temperature T in R_1 satisfies the equation given as (Nakano, 1990)

$$k(x)T' - c_1 f_{10} T = -k_0 \alpha_0 . \tag{10a}$$

The solution of eq 10a is approximately given as

$$T(x) = -\alpha_0\left[(x - n_0) + \frac{1}{2}(\beta_0 - \eta)(x - n_0)^2\right] \tag{10b}$$

$$T_1 = -\alpha_0 a(\delta) \tag{10c}$$

$$T'(n_1^-) = -\alpha_0 b(\delta) \tag{10d}$$

where $T'(n_1^-)$ is the limiting value of $T'(x)$ as x approaches n_1 while x is in R_1, and a, b and β_0 are defined as

$$a(\delta) = \delta + (1/2)(\beta_0 - \eta)\delta^2 + \ldots \tag{11a}$$

$$b(\delta) = (1 + \eta\delta)^{-1}[1 + \beta_0\delta + \ldots] \tag{11b}$$

$$\beta_0 = c_1 f_{10} / k_0 . \tag{11c}$$

We derived the following equation of heat balance in R_1 given as

$$k_1 \alpha_1 = k_0 \alpha_0 + (L - c_2 T_1) f_{10} \tag{12}$$

The mass flux of water f_{10} satisfies the equations (Nakano 1990) given as

$$P_{10} = P_{1n} - [(f_{10}/K_0) + p_0]\delta_0 \tag{13a}$$

$$P_{21} = P_{10} - f_{10} \int_{n0}^{n1} K_1^{-1}\, dx - \int_{n0}^{n1} K_1^{-1} K_2 T' dx \tag{13b}$$

where $P_{10} = P_1(n_0)$, $P_{1n} = P_1(n)$

n = some point in R_0

K_0 = the hydraulic conductivity in R_0

p_0 = gravity term, density $d_1 \times$ gravitational acceleration

$$\delta_0 = n_0 - n \geq 0. \tag{13c}$$

In order to reduce eq 13b to a simpler form, we introduced (Nakano and Takeda 1991) the following two dimensionless quantities:

$$\phi_0(T) = T^{-1} \int_0^T (K_{10}/K_1)(K_2/K_{20})\, dT \tag{14a}$$

$$\phi_1(T) = T^{-1} \int_0^T (K_{10}/K_1)(k/k_0)\, dT \tag{14b}$$

where K_{10} and K_{20} are the limiting values of K_1 and K_2, respectively, as x approaches n_0 while x is in R_1. We obtained (Nakano and Takeda 1991) the following equations given as

$$K_0 = K_{10} \tag{15a}$$

$$\gamma = K_{20}/K_0 \tag{15b}$$

$$\phi_{01} = 1, \qquad \text{if } f_{10} = 0 \tag{15c}$$

$$-T_1 = \left(\sigma + \delta_0 K_0^{-1} f_{10}\right) / I \tag{16a}$$

$$I = \gamma \phi_{01} - K_0^{-1} y \phi_{11} \tag{16b}$$

$$\sigma = P_{21} - P_{1n} \tag{16c}$$

where ϕ_{01}, ϕ_{11} and y are defined as

$$\phi_{01} = \phi_0(T_1) \tag{17a}$$

$$\phi_{11} = \phi_1(T_1) \tag{17b}$$

$$y = f_{10}/\alpha_0. \tag{17c}$$

Equation 15a holds true because the composition of the freezing soil is continuous at n_0, and eq 15b and c follow from eq 4b.

For the sake of convenience we will reduce eq 16a to a form similar to eq 3b. First, we will introduce the following four dimensionless quantities:

$$\omega_0 = \begin{cases} 0, & T_1^{**} = 0 \\ \left(-T_1^{**}\right)^{-1} \displaystyle\int_0^{T_1^{**}} \left[1 - K_2(\gamma K_1)^{-1}\right] dT, & T_1^{**} < 0 \end{cases} \tag{18a}$$

$$\omega_1 = \begin{cases} 1, & T_1 = T_1^{**} \\ (-\Delta T)^{-1} \displaystyle\int_{T_1^{**}}^{T_1} \left[(K_0 K_2)(K_1 K_{20})^{-1}\right] dT, & T_1 < T_1^{**} \end{cases} \tag{18b}$$

$$\omega_2 = \begin{cases} 0, & T_1^{**} = 0 \\ \left(-T_1^{**}\right)^{-1} \displaystyle\int_0^{T_1^{**}} \left[1 - kK_0(k_0 K_1)^{-1}\right] dT, & T_1^{**} < 0 \end{cases} \tag{18c}$$

$$\omega_3 = \begin{cases} 1, & T_1 = T_1^{**} \\ -\Delta T^{-1} \displaystyle\int_{T_1^{**}}^{T_1} kK_0(k_0 K_1)^{-1} dT, & T_1 < T_1^{**} \end{cases} \tag{18d}$$

Using eq 18a–d, we will write ϕ_{01} and ϕ_{11} as

$$T_1\phi_{01} = T_1^{**}(1 + \omega_0) - \omega_1 \Delta T \tag{19a}$$

$$T_1\phi_{11} = T_1^{**}(1 + \omega_2) - \omega_3 \Delta T. \tag{19b}$$

According to M_1 the mass flux of water f_{10} in a neighborhood of n_1 in R_1 is given as (Nakano and Takeda 1991)

$$f_{10} = -K_{11} P_1'(n_1^+) + bK_{21}\alpha_0 \tag{20}$$

where K_{11} and $P_1'(n_1^+)$ are the limiting values of K_1 and P_1', respectively, as x approaches n_1 while x is in R_1. We will rewrite eq 20 as

$$y = K_{21}\varphi_0 \tag{21a}$$

$$\varphi_0 = b - K_{11} P_1'(n_1^+)(\alpha_0 K_{21})^{-1}. \tag{21b}$$

We found (Nakano and Takeda 1991) that $P_1'(n_1^+)$ is positive in R_s and vanishes on R_s^*; namely

$$P_1'(n_1^+) > 0 \quad \text{in} \quad R_s \tag{22a}$$

$$P_1'(n_1^+) = 0 \quad \text{on} \quad R_s^*. \tag{22b}$$

From eq 22a, 22b and 21b we obtain

$$\varphi_0 = b \quad \text{on} \quad R_s^* \tag{23a}$$

$$b > \varphi_0 > 0 \quad \text{in} \quad R_s \tag{23b}$$

$$\varphi_0 = 0 \quad \text{on} \quad R_s^{**}. \tag{23c}$$

Using eq 21a, we will reduce eq 16b to

$$I = \gamma(\phi_{01} - \gamma_1\varphi_0\phi_{11}) \tag{24a}$$

where γ_1 is defined as

$$\gamma_1 = K_{21}K_{20}^{-1}. \tag{24b}$$

Substituting ϕ_{01} and ϕ_{11} in eq 24a by eq 19a and b and using eq 1, we will reduce eq 24a to

$$-T_1 I = \sigma[1 + \omega_0 - \gamma_1\varphi_0(1 + \omega_2)] + \gamma[\omega_1 - \gamma_1\varphi_0\omega_3]\Delta T. \tag{25a}$$

Combining eq 25a with 16a, we obtain

$$\delta_0 K_0^{-1} f_{10} + [\gamma_1\varphi_0(1 + \omega_2) - \omega_0]\,\sigma = \gamma[\omega_1 - \gamma_1\varphi_0\omega_3]\Delta T. \tag{25b}$$

Now we will reduce eq 25b to a form similar to eq 3b as

$$\Delta T = \hat{a}_0 + \hat{a}_1 f_{10} \tag{25c}$$

where $\hat{a}_0$ and $\hat{a}_1$ are defined as

$$\hat{a}_0 = [\gamma_1\varphi_0(1 + \omega_2) - \omega_0]\,\sigma(\gamma\varphi_1)^{-1} \tag{25d}$$

$$\hat{a}_1 = \delta_0(\gamma K_0\varphi_1)^{-1} \tag{25e}$$

$$\varphi_1 = \omega_1 - \gamma_1\varphi_0\omega_3. \tag{25f}$$

We will examine eq 25c for a special case where f_{10} is very small. It follows from eq 21a that φ_0 vanishes as f_{10} vanishes. We find from eq 18a that ω_0 vanishes because of eq 4b as f_{10} vanishes. It follows from eq 1 that T_1 approaches T_1^{**}; hence, ω_1 approaches one as f_{10} approaches zero. Hence, $\hat{a}_0$ approaches zero and $\hat{a}_1$ approaches $\delta_0(\gamma K_0)^{-1}$ as f_{10} approaches zero. Therefore, when f_{10} is very small, eq 25c may be approximately given as

$$\Delta T = \hat{a}_1 f_{10}. \tag{26}$$

Since f_{10} is the growth rate of the ice layer, eq 26 states that the growth rate of the ice layer is proportional to the degree of supercooling and that the rate coefficient $(\hat{a}_1)^{-1}$ depends on the hydraulic properties of R_0 and R_1, namely the availability of unfrozen water. Equation 26 is consistent with the theory of crystal growth in supercooled liquid (Chalmers 1964).

We will define the thicknesses δ_e of R_{11} and δ^{**} of R_{10} (Fig. 2) as

$$\delta_e = n_1 - n_{10} \tag{27a}$$

$$\delta^{**} = n_{10} - n_0 \, . \tag{27b}$$

Then the thickness δ of R_1 is obviously given as

$$\delta = \delta^{**} + \delta_e \, . \tag{27c}$$

Using eq 10c, we obtain

$$T_1^{**} = -\alpha_0 a\,(\delta^{**}). \tag{27d}$$

Using eq 10c and 11a, we obtain

$$\Delta T = \alpha_0 a_e \tag{27e}$$

where a_e is defined as

$$a_e = a(\delta) - a(\delta^{**}) \tag{27f}$$

$$= \delta_e + \frac{1}{2}\,(\beta_0 - \eta)\,(\delta_e + 2\delta^{**})\,\delta_e + \dots \, . \tag{27g}$$

Using eq 27e, we will reduce eq 26 to

$$a_e = \hat{a}_1 y \tag{28a}$$

where $\hat{a}_1$ may be written as

$$\hat{a}_1 = \delta_0(\gamma K_0)^{-1}\left(\omega_1 - K_{20}^{-1}\omega_3 y\right)^{-1}. \tag{28b}$$

When f_{10} is small, y and δ_e are also small and eq 28a and b are reduced to

$$\delta_e = \hat{a}_1 y \tag{29a}$$

$$\hat{a}_1 = \delta_0\,(\gamma K_0 \omega_1)^{-1} \, . \tag{29b}$$

From eq 29a and b we find that the thickness of the essential frozen fringe is proportional to y and that the essential frozen fringe vanishes as f_{10} vanishes. In other words, when f_{10} is very small, we may state that the appearance of an essential frozen fringe is induced by the flow of unfrozen water regardless of σ. This implies that an essential frozen fringe appears only under a dynamic condition.

MODEL M_1 AND SEGREGATION POTENTIAL

We will show below that M_1 is consistent with eq 2a, which was found empirically by Konrad and Morgenstern (1980, 1981) and was confirmed by Ishizaki and Nishio (1985). In a typical experiment

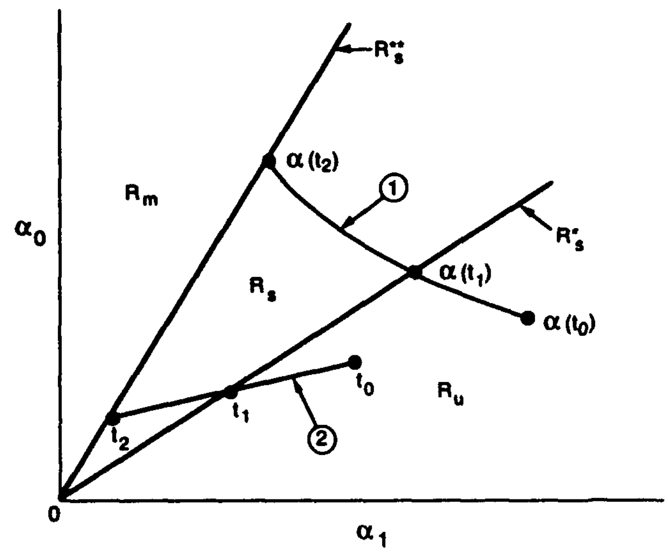

Figure 4. Schematic of trajectories $\alpha(t)$ that approximately describe the condition of freezing at the formation of the final ice lens.

by Konrad and Morgenstern (1981), the temperature field in the system changes rapidly at the start of the experiment. However, as time elapses, the rate of the change slows down so that the transient freezing may be accurately approximated by a series of successive steady states. Hence, the later part of the experiment can be approximately represented by trajectory 1 in Figure 4, consisting of points $\alpha(t) = \{\alpha_1(t), \alpha_0(t)\}$ for $t_2 \geq t \geq t_0$.

A point $\alpha(t_0)$ is in R_u where frozen soil without any visible ice layer grows. As α_1 decreases and α_0 increases, the trajectory approaches the vicinity of a point $\alpha(t_1)$ in R_u. As we described previously (Takeda and Nakano 1990) the pattern of ice-rich frozen soil grown in this vicinity evidently depends on the soil type and the magnitude of α_1 (or α_0). The results of tests on Kanto loam, for instance, clearly indicate that the pattern of rhythmic ice banding is formed at the small values of α_1 while soil particles or small aggregates of soil particles are evenly dispersed at the greater values of α_1.

When $\alpha(t)$ reaches the point $\alpha(t_1)$ on R_s^*, the final ice layer emerges. While $\alpha(t)$ moves toward the point $\alpha(t_2)$ on R_s^{**}, the growth of the final ice layer continues with the decreasing growth rate until $\alpha(t)$ reaches the point $\alpha(t_2)$ on R_s^{**} where the ice layer stops growing. It should be noted that a line of constant f_{10} is nearly parallel to R_s^{**} because of eq 12. From eq 20 and 22b we obtain on R_s^*

$$f_{10}^* = y^* \alpha_0 = K_{21}^* b \alpha_0 \qquad \text{on } R_s^*. \tag{30}$$

It follows from eq 30 that the water intake flux, f_{10}^*, at the formation of the final ice layer is proportional to the temperature gradient, $b\alpha_0$, at n_1^+. Comparing eq 30 with 2a, we find that SP_0 and $(T')_a$ in eq 2a correspond to K_{21}^* and $-b\alpha_0$ in eq 30, respectively. Since the temperature gradient in R_1 does not vary significantly, the segregation potential SP_0 is nothing but K_{21}^* (the limiting value of the transport function K_2 as x approaches n_1 while x is in R_1 at the formation of the final ice layer), when a point $\alpha(t)$ is on R_s^* in the diagram of temperature gradients, namely

$$SP_0 = K_{21}^* = y^* b^{-1}. \tag{31}$$

We have shown that M_1 is consistent with eq 2a. It is clear from eq 20 that eq 30 holds true on R_s^* but does not hold in R_s because of eq 22a. In other words, the value of y defined by eq 17c is equal to bK_{21}^* on R_s^*. However, the value of y in R_s depends on a specific trajectory $\alpha(t)$. For instance, on trajectory 1 in Figure 4 the value of y decreases from bK_{21}^* as $\alpha(t)$ moves toward the point $\alpha(t_2)$ from the point $\alpha(t_1)$ and vanishes at the point $\alpha(t_2)$. On this trajectory f_{10} decreases with the increasing α_0. However, it is easy to see that f_{10} decreases with the decreasing α_0 on trajectory 2 for $t_2 > t > t_1$. Therefore, M_1 is also consistent with the empirical finding by Ishizaki and Nishio (1985) that the value of y_a varies widely and that f_{10} may either increase or decrease with the increasing α_0 depending on a given specific trajectory. This finding by Ishizaki and Nishio (1985) was empirically confirmed (Nakano and Takeda 1991) when $\sigma = 0$.

According to our definition K_{21}^* is the value of K_{21} evaluated on R_s^*. Since any point on R_s^* is uniquely specified by eq 8b, we may write K_{21}^* as

$$K_{21}^* = K_{21}^*(\alpha_0; \delta_0, P_{1_n}, \sigma). \tag{32}$$

We studied (Nakano and Takeda 1991) the dependence of K_{21}^* on α_0 for a special case where $\delta_0 = 2.0$ cm, $P_{1n} = 0.1$ MPa and $\sigma = 0$ for three types of soils. It was found that K_{21}^* is nearly constant for a g soil if α_0 is greater than 2.0 (°C cm^{-1}). However, K_{21}^* tends to increase with decreasing α_0 in the of α_0 with 2.0 (°C cm^{-1}) > α_0 > 0 for the two types of soils, Tomakomai silt and Fujinomori Unfortunately, we were unable to confirm behavior similar to this of K_{21}^* for Kanto loam because of a lack of data. Using the additional data newly obtained, we will show such behavior for Kanto loam below.

Konrad and Morgenstern (1980, 1981, 1982) empirically found eq 2b that is equivalent to the following equation given as

$$K_{21}^* = K_{21}^*(P_{10}^*, \sigma) \tag{33}$$

where an asterisk for P_{10} is used to emphasize that the value of P_{10} is evaluated when a point $\alpha(t)$ is on R_s^*. Since their hydraulic conditions were not specified in the same manner as in our experiments, we will reduce eq 33 to the form appropriate to our system. In our system P_{10} is given by eq 13a. Hence, we obtain

$$P_{10}^* = P_{1_n} - \left[\left(f_{10}^* / K_0\right) + p_0\right] \delta_0 \tag{34}$$

where f_{10}^* is the value of f_{10} on R_s^* and is uniquely determined by α_0 (eq 8b) if δ_0, P_{1_n} and σ are given. Therefore, P_{10}^* in eq 33 can be replaced by α_0, δ_0 and P_{1_n} so that eq 33 is reduced to eq 32. We have shown that M_1 is consistent with eq 2b, which was found empirically by Konrad and Morgenstern (1980, 1981, 1982).

Konrad and Morgenstern (1981) empirically found that SP_0 is a monotonically decreasing function of $-P_{10}^*$ when $\sigma = 0$. Since P_{10}^* represents the combined effects of α_0, δ_0 and P_{1_n}, in order to find the effect of the temperature gradient, we plotted the data of SP_0 vs. $(-T')_a$ obtained by Konrad and Morgenstern (1981) in Figure 5, where the number assigned to each data point corresponds to the test number of their E series experiments. The data points E4 through 7 were obtained for a single layer of Devon silt under various temperature conditions. These data points clearly indicate that SP_0 tends to increase with the decreasing temperature gradient. This tendency is consistent with our empirical findings. Tests E8 and E9 were both two-layer systems in which the hydraulic conductivities K_0 of the unfrozen bottom layers were, respectively, higher and lower than that

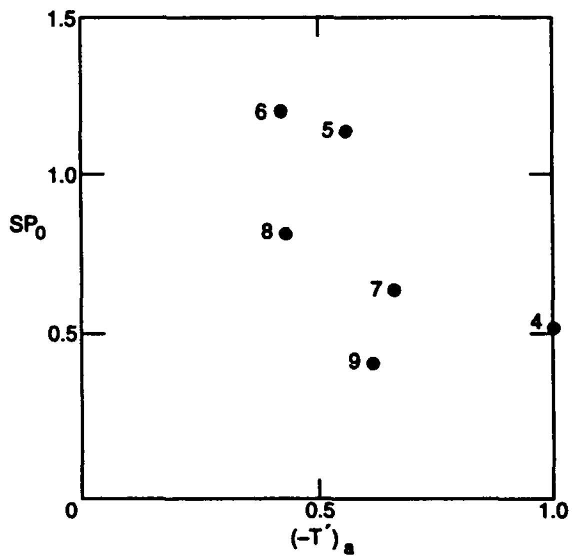

Figure 5. Values of SP_0 *[g(cm °C d)$^{-1}$] vs. the values of the average temperature gradient* $(-T')_a$ *(°C cm^{-1}) obtained by Konrad and Morgenstern (1981).*

of the unfrozen Devon silt. Since the temperature gradients in these two tests were not equal, the effects of hydraulic conditions alone on SP_0 are difficult to assess.

RESULTS OF DATA ANALYSIS

Steady growth condition

We will examine the validity of the model M_1 under the applied pressure by using the experimental data presented in Part I (Takeda and Nakano 1993). We found empirically that the steady growth region $R_s(\sigma)$ under a given applied pressure σ is approximately described as

$$\alpha_u = A\alpha_f, \qquad k_1 k_0^{-1} > A > S(\sigma) \tag{35}$$

where α_u = absolute value of the temperature gradient near n_0 in R_0
α_f = absolute value of the temperature gradient near n_1 in R_2
S = property of a given soil that depends on the applied pressure σ.

The temperature profiles in the frozen and the unfrozen parts are not exactly linear when the steady growth of an ice layer is taking place because of the convective heat transport. However, the amount of heat transported by convection is much less than that transported by conduction. The difference between α_u (or α_f) and α_0 (or α_1) is negligibly small as shown empirically and theoretically in Nakano and Takeda (1991). Therefore, eq 35 is nearly equivalent to

$$\alpha_0 = A\alpha_1, \qquad -k_1 k_0^{-1} > A > S(\sigma). \tag{36}$$

We will no longer discriminate α_u (or α_f) from α_0 (or α_1) in the following discussion.

According to M_1 the steady growth region $R_s(\sigma)$ under a given applied pressure σ is given by eq 5. Using y^*, we will reduce eq 5 to a form similar to eq 36 as

$$\alpha_0 = A\alpha_1, \qquad k_1 k_0^{-1} > A > k_1\left(k_0 + Ly^*\right)^{-1}. \tag{37}$$

Comparing eq 37 with 36, we find that M_1 is consistent with the experimental data if the following relation holds:

$$S(\sigma) \geq k_1\left[k_0 + Ly^*(\sigma)\right]^{-1}. \tag{38a}$$

We will define $\bar{y}^*$ as

$$S(\sigma) = k_1\left[k_0 + L\bar{y}^*(\sigma)\right]^{-1}. \tag{38b}$$

Then, it is easy to see that eq 38a is equivalent to the following relation:

$$y^*(\sigma) \geq \bar{y}^*(\sigma). \tag{38c}$$

We will examine the validity of eq 38c below.

For a given σ the value of $y^*(\sigma)$ can be calculated by using the calculated value of f_{10} based on either the measured rate of heave r or the measured rate of water intake, and the measured value of α_0 at each data point (α_1, α_0) on R_s^*. The calculated values of $y^*(\sigma)$ are plotted vs. α_0 with σ being a parameter in Figure 6. The mass flux of water f_{10} decreases by the order of 10^{-2} as σ increases from zero to 195 kPa. As the result the accuracy of measuring f_{10} tends to decrease with increasing σ and the variability of data points becomes more pronounced with increasing σ, as shown in Figure 6.

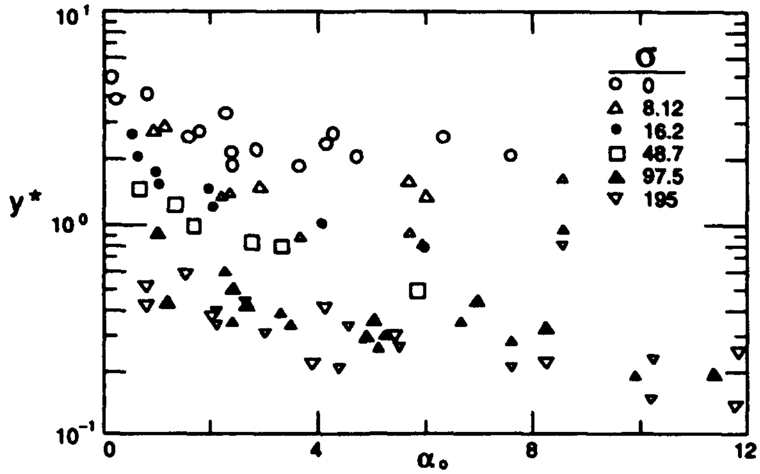

Figure 6. Values of y^* [g(cm °C d)$^{-1}$] vs. α_0 under various applied pressures σ (kPa).

Because of such variability and the limited numbers of data under $\sigma = 390$ kPa, we decided not to use the data taken under $\sigma = 390$ kPa in our analysis. From Figure 6 we find the general trend that y^* decreases with increasing σ and that y^* increases with the decreasing α_0 in the range of $\alpha_0 < 2.0$ °C cm^{-1}. The latter trend was also observed (Nakano and Takeda 1991) in the experiments with Tomakomai silt and Fujinomari clay under null applied pressure.

We calculated the values of $\bar{y}^*(\sigma)$ from the values of $S(\sigma)$ that were presented in Table 2 of Part I (Takeda and Nakano 1993). We also calculated the average of $y^*(\sigma)$ over all the data points obtained for each σ. The values of $\bar{y}^*(\sigma)$ and the average values $y_a^*(\sigma)$ of $y^*(\sigma)$ for each σ are presented in Table 1. It is clear from Table 1 that eq 38c does not hold for every σ, particularly for greater values of σ. However, the average values $y_a^*(\sigma)$ do not differ significantly from those of $y^*(\sigma)$. We may conclude that the model M_1 is consistent with the experimental data regardless of σ and that the steady growth region of an ice layer under various applied pressures can be described by eq 37.

In order to find the dependence of y_a^* on σ, we plotted y_a^* in the logarithmic scale against σ in Figure 7. It is clear from the figure that y_a^* is a decreasing function of σ. Assuming that b is nearly equal to one, we may conclude that K_{21}^* (or SP_0) is a decreasing function of σ, which was found

Table 1. Calculated values $\bar{y}^*$ [g (cm °C d)$^{-1}$] and the average measured values y_a^* under various applied pressures σ (kPa).

	Applied pressures (σ)					
	0.0	*8.12*	*16.2*	*48.7*	*97.8*	*195*
$\bar{y}^*$	2.34	2.12	1.14	1.12	0.72	0.56
y_a^*	2.86	1.98	1.61	0.97	0.45	0.35

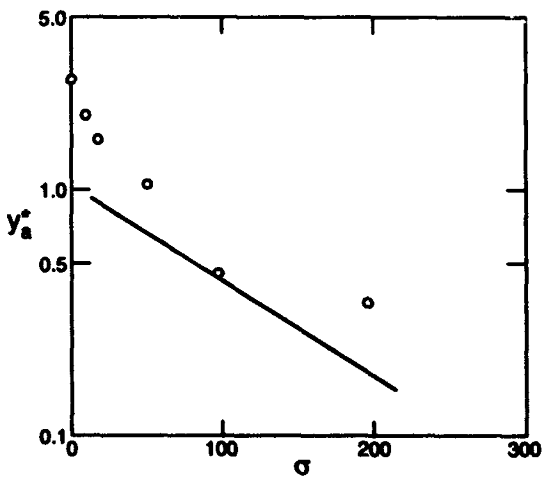

Figure 7. Average values y_a^* [g(cm °C d)$^{-1}$] vs. σ (kPa) where a solid line is the empirically determined relationship for Devon silt obtained by Konrad and Morgenstern (1982).

empirically by Konrad and Morgenstern (1982). Their data with Devon silt were presented in the functional form given as

$$SP_0 = a_2 \exp(-a_3\sigma). \tag{39}$$

When we use the same units of SP_0 and σ as those of $y_a{}^*$ and σ in Figure 7, the values of the constants a_2 and a_3 are 1.04 and 8.95×10^{-3}, respectively, and eq 39 is presented by the straight line in Figure 7. Because of the limited number of data points it is not certain that our data can be presented in the same functional form as eq 39. However, the important point is that K_{21}^* is a decreasing function of σ. The reason for such dependence will be discussed below.

Dependence of y^* on T_1^*

Combining eq 30 with eq 32, we obtain

$$y^* = bK_{21}^*(\alpha_0; \delta_0, P_{1_n}, \sigma). \tag{40a}$$

For a special case such as our experiments where δ_0 and P_{1_n} are specified, we may reduce eq 40a to:

$$y^* = bK_{21}^*(\alpha_0, \sigma). \tag{40b}$$

On the other hand K_{21}^* is the value of K_{21} when a point (α_1, α_0) is on R_s^*. From eq 4e we obtain

$$K_{21}^* = K_{21}^*(T_1^*, \rho) \tag{40c}$$

where T_1^* is the temperature at n_1 when a point (α_1, α_0) is on R_s^*. It is clear from eq 40b and c that T_1^* and the composition ρ generally depend on α_0 and σ. We will study empirically the relationship between y^* and T_1^* below.

Using the set of data obtained under the applied pressure of 48.7 kPa as an example, we will describe how we obtained the empirically determined value of T_1^* from the data. The results of our data analysis are presented in Table 2, where n_1 is the observed location of the interface between R_1 and R_2, while n_0 is the location of the 0°C isotherm calculated by using the measured temperature profile in R_0. The values of δ in the table are calculated simply from eq 9d and vary between 0.91 and 1.5 mm. We have found that the value of δ increases with the increasing σ and that the maximum value of δ in the range of $\sigma \le 195$ kPa is 4.8 mm under the condition of $\alpha_0 = 0.80$ and $\sigma = 195$ kPa.

The value of T_1^* can be calculated from either the measured temperature profile in R_0 or that in R_2. As we discussed in Part I (Takeda and Nakano 1993), the temperature measurements in R_0 are more accurate than those in R_2. Therefore, it is desirable to determine T_1^* from the profile in R_0. However, the thermal conductivity $k(x)$ in R_1 is unknown because the composition of R_1 is unknown. According to the model M_1, T_1 is given by eq 10c and 11a. Hence, when the variation of k in R_1 is small, T_1^* is nearly equal to T_{10} defined as

Table 2. Summary of data analysis with σ = 48.7 kPa.

Exp.	α_0 (°C cm^{-1})	f_{10}^* (g cm^{-2} d^{-1})	y^* [g (cm °C d)$^{-1}$]	n_1 (cm)	n_0 (cm)	δ (cm)	$-T_{10}$ (°C)	$-T_{11}$ (°C)	$-\hat{T}_1^*$ (°C)
1	0.642	0.968	1.51	0.67	0.55	0.12	0.076	0.174	0.125
2	1.29	1.59	1.23	0.25	0.099	0.15	0.192	0.198	0.195
3	1.62	1.60	0.988	0.28	0.13	0.15	0.239	0.211	0.225
4	2.76	2.13	0.770	0.18	0.086	0.094	0.260	0.245	0.255
5	3.29	2.65	0.804	0.20	0.080	0.12	0.378	0.320	0.349
6	5.85	2.97	0.507	0.13	0.039	0.091	0.535	0.467	0.501

$$T_{10} = -\alpha_0\delta. \tag{41a}$$

It is clear from eq 10c and 11a that T_1^* is accurately approximated also by T_{10} when δ is very small. The calculated values of T_{10} are listed in Table 2. When σ is negligible, Nakano and Takeda (1991) found that $k(x)$ tends to increase with x in R_1. Therefore, T_{10} would be a lower bound of T_1^*, namely

$$T_1^* \geq T_{10}. \tag{41b}$$

We also calculated the value of T_1^* from the measured profile in R_2. The calculated values, which are referred to as T_{11}, are listed in Table 2. We find from Table 2 that T_{10} tends to be less than T_{11}. A tendency similar to this was also found in all other cases of different applied pressures. Under these circumstances we decided to choose the average of T_{10} and T_{11} to be the empirically determined value $\widehat{T}_1^*$ of T_1^* defined as

$$\widehat{T}_1^* = 0.5\,(T_{10} + T_{11}). \tag{42}$$

The values of $\widehat{T}_1^*$ are listed in Table 2.

The values of y^* are plotted against $-\widehat{T}_1^*$ with the logarithmic scale under various applied pressures σ in Figure 8. Despite some scatter, it is clear that the relation between y^* and $\widehat{T}_1^*$ is nearly one to one. The solid line in Figure 8 is the best linear approximation to the data points given as

$$y^* = K_{21}^* = \begin{cases} K_{20} & \widehat{T}_0 < T \leq 0 \quad (43a) \\ K_{20}\left(\widehat{T}_0/T\right)^{b_2} & T \leq \widehat{T}_0 \quad (43b) \end{cases}$$

where b is assumed to be one, K_{20} is the limiting value of K_2 as x approaches n_0 while x is in R_1 and is equal to 1.98×10^3 g(cm d °C)$^{-1}$ (Nakano and Takeda 1991), $\widehat{T}_0 = -1.5 \times 10^{-4}$ °C and $b_2 = 1.039$. As we showed (Nakano and Takeda 1991), K_{20} satisfies the equation given as

$$K_{20} = \gamma K_0 \tag{44}$$

where K_0 is the hydraulic conductivity in R_0. It is easy to see that y^* becomes infinite as T approaches zero in eq 43b. Although eq 43b is the best approximation to the data points, eq 43a is needed to fit the data points in a neighborhood of $T = 0$°C.

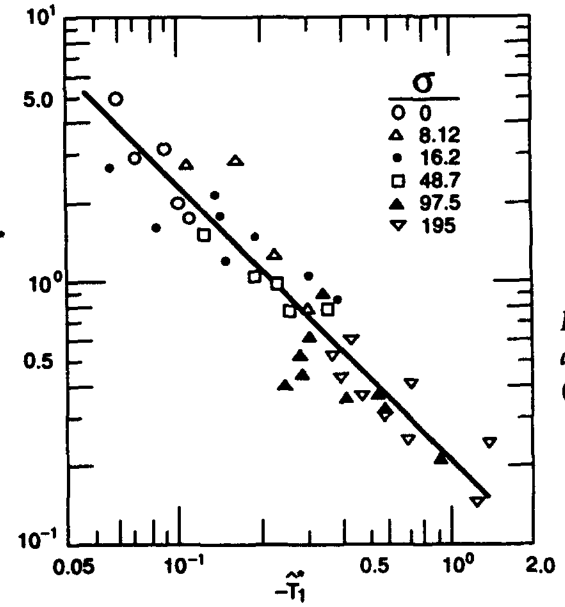

Figure 8. Values of y^* [g(cm °C d)$^{-1}$] vs. the temperature $-\widehat{T}_1^*$ (°C) under various applied pressures σ (kPa).

According to eq 40c, y^* generally depends on T_1^* and the composition ρ. However, we have found empirically that y^* depends mainly on T_1^*. This implies that the composition in a neighborhood of n_1 in R_1 is not significantly affected by σ and α_0 (or f_{10}). Since $\widehat{T_1^*}$ varies between 0 and −1.0°C in Figure 8, we may conclude that the composition of the essential frozen fringe R_{11} depends mainly on the temperature regardless of σ and f_{10}. There is another interpretation of Figure 8: that the transport function K_2 does not depend on the composition. Recently Nakano and Tice (1990) found empirically that K_2 in unsaturated frozen clay strongly depends on the composition, particularly the content of ice. Their empirical finding supports the former interpretation.

Figure 8 shows that the range of $\widehat{T_1^*}$ for a given σ shifts toward the lower temperature as σ increases. The segregation potential K_{21}^* evidently depends primarily on the temperature T_1^* at n_1 and is an increasing function of T_1^* because the applied pressure in the range of $\sigma \leq 195$ kPa does not affect significantly the composition of the essential frozen fringe R_{11}. This is the reason why the segregation potential K_{21}^* is generally a decreasing function of σ.

Dependence of T_1^* on f_{10}^*

The values of $-\widehat{T_1^*}$ are plotted against f_{10}^* under various applied pressures σ in Figure 9. Figure 9 shows that the relationship between $\widehat{T_1^*}$ and f_{10}^* is approximately linear for a given σ, which is consistent with the empirical relation (eq 3b and c) found by Ishizaki and Nishio (1985). It is clear from Figure 9 that the constants a_0 and a_1 strongly depend on σ. An important question is whether we can describe the behavior of data points in Figure 9 by eq 25c derived based on M_1. We are not able to show that eq 25c is consistent with the data because we have no data on the transport function K_1. However, we will show below that eq 25c is consistent with the data if the function K_1 is properly chosen.

The model M_1 is defined as the frozen fringe where ice may exist but does not grow, and the mass flux of water f_1 is given by eq 4a with the condition of eq 4b and c. When $\sigma > 0$, the essential frozen fringe R_{11} vanishes as f_1 vanishes but R_{10} does not. From eq 4b we obtain:

$$K_2/K_1 = \gamma \qquad \text{in } R_{10} \text{ if } f_1 = 0. \tag{45}$$

When the steady growth of an ice layer occurs, f_1 remains constant at f_{10} throughout R_0, R_{10} and R_{11}. An important question arises: whether or not eq 45 holds true when f_{10} does not vanish. In other

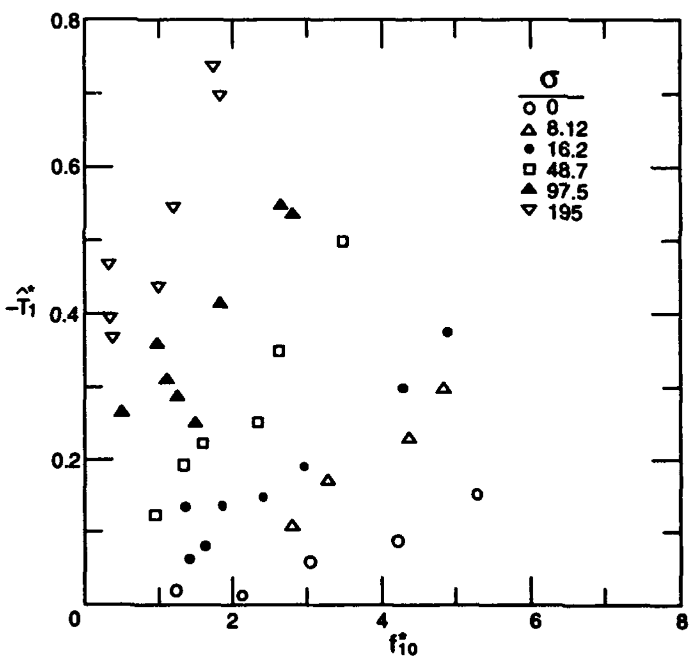

Figure 9. Values of $-\widehat{T_1^*}$ (°C) vs. the mass flux of water f_{10}^* [g (cm^{-2} d^{-1})] under various applied pressures σ (kPa).

words, is the composition of R_{10} significantly affected by f_{10}? As we described above, our data indicate that neither σ nor f_{10} significantly affects the composition of the essential frozen fringe. Therefore, it is probable that the effect of f_{10} on the composition of R_{10} is negligible. We will assume that eq 45 holds true regardless of f_{10}, namely

$$K_2/K_1 = \gamma \qquad \text{in } R_{10}. \tag{46}$$

When eq 46 holds true, the dimensionless quantity ω_0 defined by eq 18a vanishes. Hence, eq 25d is reduced to

$$\hat{a}_0 = \gamma_1 \varphi_0 (1 + \omega_2)\, \sigma\, (\gamma \varphi_1)^{-1}. \tag{47}$$

Now we will calculate T_1^* as a function of f_{10}^* by eq 25c as follows. Since T_1^* is the value of T_1 on R_s^*, φ_0 is equal to b by eq 23a. We will assume that $b = 1$, or equivalently $k(x) = k_0$ in R_1. We also assume that $K_2(T)$ is equal to $K_{21}^*(T)$ given by eq 43a and b. The value of T_1^{**} is calculated by eq 1 for a given σ. Horiguchi and Miller (1983) found empirically that the transport functions $K_1(T)$ of various soils can accurately be represented in the same functional form as eq 43b. We will assume that $K_1(T)$ is given as

$$K_1(T) = \begin{cases} K_0 & \hat{T}_0 < T \le 0 \\ K_0 \left(\hat{T}_0 / T\right)^{b_1} & T \le \hat{T}_0 \end{cases} \tag{48}$$

where K_0 is the hydraulic conductivity in R_0 and is 1.77×10^3 g(cm d MPa)$^{-1}$ (Nakano and Takeda 1991). The value of $\hat{T}_0$ is the same as used in eq 43a and b. A constant b_1 is an unknown parameter to be determined.

As we described in Part I (Takeda and Nakano 1993), the applied pressure σ affects the void ratio e of a specimen. Although the variation of e itself is negligibly small, the hydraulic conductivity K_0 may be affected significantly. Therefore, we determined empirically the relationship between K_0 and σ given as

$$K_0(\sigma) = 1.77 \times 10^3\, \sigma^{-0.1088} \tag{49}$$

where the units of K_0 and σ are g(cm d MPa)$^{-1}$ and kPa, respectively. The value of K_0 is reduced to about one-half according to eq 49 when σ is increased from zero to 195 kPa. The functional form of eq 49 is consistent with the data obtained by Fukushima and Ishii (1986). In our calculations of T_1^* for $\sigma > 0$ we used $K_0(\sigma)$ given by eq 49 instead of the value of K_0 at $\sigma = 0$.

Now we can calculate $T_1^*(f_{10})$ with b_1 being a parameter. Calculating $T_1(f_{10})$ in the wide range of b_1, we find that the calculated curves $T_1^*(f_{10})$ fit the data well if b_1 is about one-half of b_2. The calculated curves with $b_1 = 0.52$ are presented in Figure 10 together with the data. If b_1 is decreased (or increased) from this value, then the gradients of these curves, $d(-T_1^*)/df_{10}^*$, increase (or decrease). We have shown that eq 25c is consistent with the data if the function K_1 is given by eq 48 with $b_1 = 0.52$.

DISCUSSION AND CONCLUSIONS

Many models of frost heave have been proposed in the past (Nakano 1990). However, the model proposed by Konrad and Morgenstern (1982) is one of few that were built on an empirical base. Their segregation potential theory was easily adapted to solve engineering problems in the past. As our quantitative understanding on the subject is increased, their model can be improved or refined without sacrificing its easy adaptability to engineering problems.

Konrad and Morgenstern (1981) proposed an equation similar to eq 4a where the mass flux of water f_1 is given as the sum of two terms, namely, a pressure-related term and a temperature related

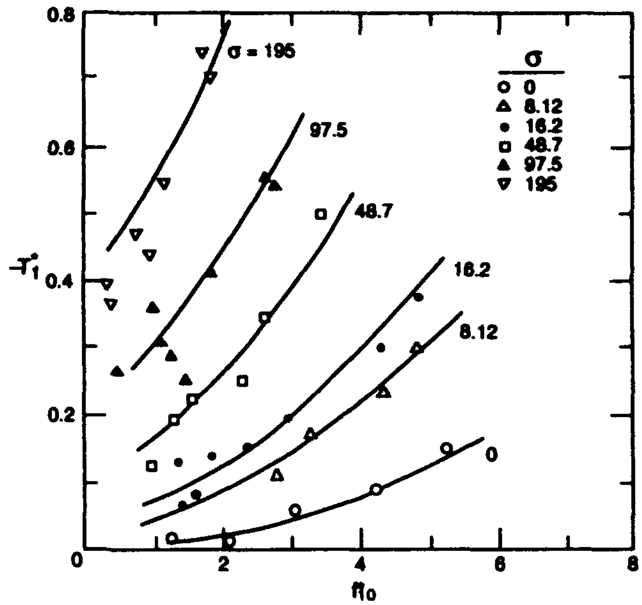

Figure 10. Values of $-\widehat{T}_1^*$ (°C) vs. the flux f_{10}^* [g (cm^{-2} d^{-1})] where solid curves are predicted relationships between these two variables by eq 25c under various applied pressures σ (kPa).

term. However, curiously enough, they dropped the pressure term in their later publications. Since the pressure term in eq 4a is generally negative according to M_1, the omission of this term leads to overestimating f_1. Therefore, their model certainly predicts an upper bound of frost heave as they claim (Konrad and Morgenstern 1982). However, some serious criticisms against their model cannot be refuted unless the pressure term is restored, as we will explain below.

When the pressure term is neglected, it is clear from eq 4a that f_1 is nonnegative. This is the reason why Konrad and Morgenstern (1982) could not provide a satisfactory explanation for the expulsion of water from freezing soils. Takashi et al. (1978) conducted a series of frost heave tests in which the temperature in the unfrozen part R_0 was kept constant at 0.2–0.3°C higher than the freezing point of specimens. In other words, the positive temperature term of eq 4a was kept small in their tests.

The absolute value of the negative pressure term of eq 4a is small when the applied pressure σ is small. Hence, f_1 can be positive when σ is small. However, the pressure term decreases with the increasing σ and f_1 vanishes at certain values of σ because the two terms of eq 4a cancel out. As σ increases beyond this value, f_1 becomes negative; that is, the expulsion of water from freezing soils takes place. Takashi et al. (1978) found empirically what we described above.

Another serious criticism of the segregation potential theory was raised by Ishizaki and Nishio (1985) that the value of y_a defined by eq 3a is constant strictly at the instant when the final ice lens emerges, but except for this instant, y_a varies widely during the growth period of the final ice lens. As we explained earlier, the pressure term of eq 4a vanishes at the formation of the final ice lens, but the negative pressure term varies depending on a specific trajectory in the diagram of temperature gradients when the final ice lens is growing. The empirical finding by Ishizaki and Nishio (1985) can be explained if the pressure term is restored. Assuming that the temperature $T_1^*(\sigma)$ at the formation of the final ice lens depends mainly on the property of a given soil alone, Konrad and Morgenstern (1982) termed $T_1^*(\sigma)$ as the "segregation freezing temperature." However, we have found empirically (Fig. 9) that $T_1^*(\sigma)$ depends strongly on the mass flux f_{10}^*.

Using the data obtained in Part I (Takeda and Nakano 1993), we evaluated the accuracy of M_1. We found that the predicted steady growth condition of an ice layer under various applied pressures is in good agreement with that found empirically. We also found that M_1 is consistent with the data obtained by Konrad and Morgenstern (1980, 1981, 1982) that were used to support their segregation potential theory. Their method of frost heave prediction is a sound and useful tool for engineering problems that consistently provides an upper bound of frost heave. However, the accuracy of their method can be significantly improved and some of the serious criti-cisms against it can be refuted if the pressure term in the equation of water flow is restored as we discussed above.

LITERATURE CITED

Chalmers, B. (1964) *Principles of Solidification.* New York: John Wiley & Sons.

Edlefsen, N.E. and A.B.C. Anderson (1943) Thermodynamics of soil moisture. *Hilgardia,* **15**(2): 31–298.

Fukushima, S. and T. Ishii (1986) An experimental study of the influence of confining pressure on permeability coefficients of filldam core material. *Japanese Society of Soil Mechanics and Foundations Engineering,* **26:** 32–46.

Horiguchi, K. and R.D. Miller (1983) Hydraulic conductivity functions of frozen materials. In *Proceedings, 4th International Conference on Permafrost, July 17–22, Fairbanks, Alaska.* Washington, D.C.: National Academy Press, p. 504-508.

Ishizaki, T. and N. Nishio (1985) Experimental study of final ice lens growth in partially frozen saturated soil. In *Proceedings, 4th International Symposium on Ground Freezing, 5–7 August, Sapporo, Japan* (S. Kinoshita and M. Fukuda, Ed.). Rotterdam, Netherlands: A.A. Balkema, p. 71–78.

Konrad, J.M. and N.R. Morgenstern (1980) A mechanistic theory of ice lens formation in fine-grained soils. *Canadian Geotechnical Journal,* **17:** 473–486.

Konrad, J.M. and N.R. Morgenstern (1981) The segregation potential of a freezing soil. *Canadian Geotechnical Journal,* **18:** 482–491.

Konrad, J.M. and N.R. Morgenstern (1982) Effects of applied pressure on freezing soils. *Canadian Geotechnical Journal,* **19:** 494–505.

Nakano, Y. (1990) Quasi-steady problems in freezing soils: I. Analysis on the steady growth of an ice layer. *Cold Regions Science and Technology,* **17**(3): 207–226.

Nakano, Y. and K. Takeda (1991) Quasi-steady problems in freezing soils: III. Analysis on experimental data. *Cold Regions Science and Technology,* **19:** 225–243.

Nakano, Y. and A.R. Tice (1990) Transport of water due to a temperature gradient in unsaturated frozen clay. *Cold Regions Science and Technology,* **18:** 57–75.

Radd, F.J. and D.H. Oertle (1973) Experimental pressure studies of frost heave mechanism and the growth-fusion behavior of ice. In *Permafrost: The North American Contribution to the 2nd International Conference on Permafrost, Yakutsk, 13–28 July.* Washington, D.C.: National Academy of Sciences, p. 377–384.

Takashi, T., H. Yamamoto, T. Ohrai and M. Masuda (1978) Effect of penetration rate of freezing and confining stress on the frost heave ratio of soil. In *Proceedings, 3rd International Conference on Permafrost, 10–13 July. Edmonton, Alberta.* Ottawa: National Research Council of Canada, vol. 1, p. 737–742.

Takashi, T., T. Ohrai, H. Yamamoto and J. Okamoto (1981) Upper limit of heaving pressure derived by pore-water pressure measurements of partially frozen soil. *Engineering Geology,* **18:** 245–257.

Takeda, K. and Y. Nakano (1990) Quasi-steady problems in freezing soils: II. Experiment on steady growth of an ice layer. *Cold Regions Science and Technology,* **18:** 225–247.

Takeda, K. and Y. Nakano, Y. (1993) Growth condition of an ice layer in frozen soils under applied loads: I. Experiment. USA Cold Regions Research and Engineering Laboratory, CRREL Report 93-21.

REPORT DOCUMENTATION PAGE

Form Approved
OMB No. 0704-0188

1. AGENCY USE ONLY (Leave blank)

2. REPORT DATE
January 1994

3. REPORT TYPE AND DATES COVERED

4. TITLE AND SUBTITLE

Growth Condition of an Ice Layer in Frozen Soils Under Applied Loads
2. Analysis

5. FUNDING NUMBERS

PE: 6.11.02A
PR: 4A161102AT24
TA: SC
WU: F01

6. AUTHORS

Yoshisuke Nakano and Kazuo Takeda

7. PERFORMING ORGANIZATION NAME(S) AND ADDRESS(ES)

U.S. Army Cold Regions Research
and Engineering Laboratory
72 Lyme Road
Hanover, New Hampshire 03755-1290

8. PERFORMING ORGANIZATION REPORT NUMBER

CRREL Report 94-1

9. SPONSORING/MONITORING AGENCY NAME(S) AND ADDRESS(ES)

Office of the Chief of Engineers
Washington, D.C. 20314-1000

10. SPONSORING/MONITORING AGENCY REPORT NUMBER

11. SUPPLEMENTARY NOTES

Additional funding provided by Technical Research Institute, Konoike Construction Co., Ltd., Konohana, Osaka, Japan

12a. DISTRIBUTION/AVAILABILITY STATEMENT

Approved for public release; distribution is unlimited.

Available from NTIS, Springfield, Virginia 22161.

12b. DISTRIBUTION CODE

13. ABSTRACT (*Maximum 200 words*)

The results of an experimental study on the steady growth condition of a segregated ice layer under various applied pressures were presented in Part I. Using the data obtained, we evaluate the accuracy of the model M_1, and the predicted steady growth condition is found to be in good agreement with the condition found empirically. The concept of segregation potential introduced by Konrad and Morgenstern in the early 1980s is examined based on M_1. M_1 is found to be consistent with the empirical data that were used to support their segregation potential theory.

14. SUBJECT TERMS

Frost heave Frozen soils Mathematical analysis

15. NUMBER OF PAGES
27

16. PRICE CODE

17. SECURITY CLASSIFICATION OF REPORT	18. SECURITY CLASSIFICATION OF THIS PAGE	19. SECURITY CLASSIFICATION OF ABSTRACT	20. LIMITATION OF ABSTRACT
UNCLASSIFIED	UNCLASSIFIED	UNCLASSIFIED	UL

NSN 7540-01-280-5500

Standard Form 298 (Rev. 2-89)
Prescribed by ANSI Std. Z39-18
298-102